Resonant self-focusing of a cw intense light beam

Martine Le Berre
Laboratoire des Signaux et Systèmes, Plateau du Moulon, 91190 Gif-sur-Yvette, France

Elisabeth Ressayre and Andrée Tallet
Laboratoire de Photophysique Moléculaire du Centre National de la Recherche Scientifique, Université Paris—Sud, 91405 Orsay, France

(Received 27 September 1983)

A single pass of an intense cw light beam through a strongly absorbing medium can be characterized by two parameters, the input on-axis intensity normalized to the saturation value $I_{0,0}$, and the Fresnel number F for an absorption length α^{-1}. For both large $I_{0,0}$ and F, propagation can be divided in two parts: At the very beginning, the transverse profile of the beam experiences an encoding. For a beam tuned exactly on resonance, encoding reduces to a stripping of the profile from the wings to the center, progressively, as the light beam goes further into the cell. For $F \gg 1$ and $I_{0,0} \gg 1$, and both of the same order of magnitude, this stripping can be modeled by a circular aperture placed at the end of the encoding region. Afterwards, the beam is assumed to propagate in free space, its profile exhibits Fresnel interferences and on-axis enhancement. Using a perturbative treatment, the width and the location of the aperture are analytically estimated, and the model is successfully compared with numerical predictions of on-resonance self-focusing. For $I_{0,0} \lesssim F$, the stripping and free-space propagation cannot be separated because near-axis stripping coexists with large diffraction effects on the wings. This case, the best for observing cw on-resonance enhancement, would gain in a more sophisticated model, taking into account diffraction by successive apertures.

I. INTRODUCTION

Numerical simulations of Boshier and Sandle on the propagation of a cw light beam through a two-level resonant medium have recently predicted spectacular self-focusing effects.[1] Such an on-resonance reshaping was unexpected for an absorbing medium without nonlinear refractive index,[2,3] since self-focusing was known to result from a self-lensing effect of the coupled field plus atoms system. This self-lensing effect first implies the existence of a refractive index and then a transverse gradient of the refractive index.[2,3] For a cw light beam, this requires a detuning δ between the atomic transition frequency and the carrier one. In a transient regime self-focusing may happen even for vanishing δ because the time variation of the phase of the electric field induces an instantaneous detuning giving rise to a refractive index. This self-focusing of optical pulses, predicted and analyzed by Newstein and colleagues[4,5] was experimentally confirmed by Gibbs and colleagues.[6]

The purely absorptive cw self-focusing effect was interpreted as joint effects of nonlinear absorption changing the transverse profile of the beam and diffraction acting on the distorted shape.[1] Boshier and Sandle[1] (BS) pointed out that the distortions of the beam, followed through the cell, look like near-field patterns of the diffraction of the light by a circular aperture, formed by the absorbing medium.

In this paper, we are dealing with an analytical description of the on-resonance enhancement taking the results and comments of BS into account.[7] In Sec. II, the perturbation expansions[2,3,8(b),9] successfully used for predicting the cw off-resonance enhancement are extended to the BS on-resonance case. The perturbation treatments of the diffraction break down when diffraction becomes relevant. Nevertheless, they give the focus point, just defined by the penetration at which the intensity diverges. In the on-resonance case, and for the range of parameters considered by BS, the perturbation treatment exhibits the divergence of the field amplitude on the wings of the transverse profile: an enhancement is first reached outside the axis and the intensity profile exhibits a doughnut shape. The perturbation treatment breaks down from this focus and cannot simulate properly the diffraction carrying away energy from the wings of the beam to its center.[7] This particular building of the on-axis enhancement, as the beam propagates forward, requires a treatment of the diffraction allowing an accurate communication between the wings and the near-axis region of the beam profile.

Therefore, we are led, as in Ref. 8 (referred to as I), to model the effects of the nonlinear absorption and the diffraction, taking the on-resonance BS case particularly into account.[10] Typically, I displayed large reshaping effects when both the on-axis input intensity normalized to the saturation intensity for an atom $I_{0,0}$ and the Rayleigh length z_d normalized to the absorption length α^{-1}, are much larger than unity, i.e.,

$$I_{0,0} \gg 1 \ , \qquad F = \alpha z_d \gg 1 \ , \tag{1}$$

with

$$z_d = \tfrac{1}{2} k w_0^2 \ , \tag{2}$$

where k and w_0 are the wave number and the waist of the amplitude profile, respectively. This is, too, the situation described by BS. The differences between I and Ref. 1 essentially lie in the order of magnitude of $I_{0,0}$ with respect to F:[11] In I, we were dealing with

$$F \gg I_{0,0} \tag{3}$$

(and in a general manner for any detuning δ), whereas on-resonance self-focusing (OSF) is found for F of magnitude of order $I_{0,0}$. Typically we will discuss two cases, the first, or BS2 case, taken in Fig. 2 of Ref. 1,

$$F=60\ ,\quad I_{0,0}=100\ , \tag{4a}$$

and, the second one, or BS3 case, taken in Fig. 3 of Ref. 1,

$$F=500\ ,\quad I_{0,0}=225\ . \tag{4b}$$

BS2 and BS3 cases are actually contrary to the cases encountered in I. Nevertheless, the description of the distortion of the light beam through the cell can be qualitatively the same because of large $I_{0,0}$. At the beginning of the propagation through the cell, diffraction is negligible; the beam undergoes only the absorption process which displays a nonuniform behavior along its profile, because of $I_{0,0} \gg 1$. The beam is said to experience an encoding of both its amplitude and its phase (if $\delta \neq 0$). In a general manner, at a given $\alpha z \ll F$ in order that diffraction may be neglected, the intensity profile can undergo three different regimes, depending on the transverse variable. The input intensity profile $I_0(\rho)$ is assumed to have a Gaussian shape

$$I_0(\rho)=I_{0,0}e^{-2\rho^2} \tag{5}$$

with

$$\rho=\frac{r}{w_0}\ ; \tag{6}$$

then for ρ such that $I_0(\rho)$ is much larger than αz, the medium looks transparent; for $I_0(\rho) \simeq \alpha z$, there are high nonlinearities and the profile is strongly absorbed; finally, for $I_0(\rho) \ll \alpha z$, the local intensity $I(z,\rho)$ obeys the well-known Beer's law.[8]

As previously discussed in I and as it will be shown in Sec. II, large diffraction effects require large nonlinearities with respect to $I_{0,0}$ in the absorption process, i.e., for the set of coordinates (z_{st},ρ_{st}) such that

$$\alpha z_{st}=I_{0,0}e^{-2\rho_{st}^2} \tag{7a}$$

with

$$\alpha z_{st} \ll \alpha z_d$$

or

$$\frac{z_{st}}{z_d}=\frac{I_{0,0}}{F}e^{-2\rho^2} \ll 1\ . \tag{7b}$$

This latter relation allows one to distinguish the cases studied in I from those found by BS and studied here. In I, the ratio $I_{0,0}/F$ is much smaller than unity, so that inequality (7b) is fulfilled for any ρ on the beam profile. Here, it is not true for all values of ρ; inequality (7b) implies a lower bound upon ρ in order to be satisfied.

In the model in I, the nonlinear absorption affects the whole profile at the very beginning of propagation, so that the cell can be roughly divided into two parts. The first one goes from zero to an abscissa referred to in I as z_{NL},

$$\frac{z_{NL}}{z_d} \simeq \frac{I_{0,0}}{F}\ , \tag{8}$$

where the whole profile experiences encoding of its phase and of its amplitude. This latter is stripped on its whole profile and, roughly speaking, exhibits a Gaussian shape of width equal to $I_0^{-1/2}$. Afterward, from z_{NL}, diffraction works alone, revealing the encoding effect of the nonlinearities by the free-space propagation. This model has been shown to have a range of validity by comparing it to numerical simultations[11] and experiments.[9]

In the on-resonance case, the encoding reduces to a stripping of the wings of the beam profile, while the near-axis region of the profile propagates as through a transparent medium. Diffraction becomes important before the on-axis intensity is absorbed. Let us notice that this circumstance leads to an on-axis enhancement. As in I the cell can be divided into two parts. The first one from zero to an abscissa z_{st} where the beam profile undergoes stripping of its wings. This stripped profile will be approximated by a truncated Gaussian of full width $2\rho_{st}$, related to z_{st} by the law (7a). From z_{st}, the diffraction is assumed to work alone, giving rise to Fresnel interferences by a circular aperture. This model, which assumes that the atomic medium behaves like a circular aperture, leads to profiles which agree with the numerical profiles reported by BS. As will be discussed in Sec. III Fresnel interferences from z_{st} will be compared with the profiles resulting from the free-space propagation of the stripped amplitude.

In summary, the model that we propose to interpret the BS calculations[12] is qualitatively identical to I. Nevertheless, if it is justified to neglect the effects due to nonlinear absorption after z_{NL} in the model in I, because the intensity is locally smaller than unity on the whole profile, whereas it is more questionable here after z_{st}, because the near-axis intensity is still larger than unity. This problem will be discussed in Sec. III. Two situations appear. For $F \lesssim I_{0,0}$ (BS2) the aperture is large enough in order that αz_{st} is much smaller than $I_{0,0}$. Therefore, nonlinear absorption near the axis does not compete with the Fresnel interferences. In the opposite case, $F \gtrsim I_{0,0}$ (BS3), the aperture we define leads to αz_{st} not small enough with respect to $I_{0,0}$. Nonlinear absorption of the on-axis intensity can no longer be neglected after z_{st}, and the present model is too crude. This latter situation, as already seen on the BS curves, will be shown to be the best one for very large enhancement.

In Sec. II a perturbation expansion is developed and leads to an estimate of z_{st} and ρ_{st}. In Sec. III diffraction from a truncated Gaussian is discussed with respect to BS calculations as a function of z_{st} and ρ_{st}.

II. PERTURBATION TREATMENT

We are dealing with a single pass of light beam through a nonlinear medium such that the balance parameter F be-

tween absorption and diffraction is very large. The reduced Maxwell equation can be written as

$$\left[\frac{-i}{2F}\nabla_t^2+2\frac{\partial}{\partial(\alpha z)}\right]\epsilon(z,\rho)=\frac{-\epsilon(z,\rho)}{1+|\epsilon(z,\rho)|^2}\ , \tag{9}$$

where $\epsilon(z,\rho)$ is the electric field amplitude normalized to the square root of the saturation intensity:

$$I_s=\left[\frac{\mu^2}{\hbar^2}T_1T_2\right]^{-1}\ . \tag{10}$$

At the very beginning of the propagation through the cell, ($z \ll\ll z_d$) diffraction may be neglected. Therefore the field amplitude is a solution of the Maxwell equation (9) without the diffraction term ∇_t^2. It is the implicit solution first given by Icsevgi and Lamb[13] and referred to as the encoded function here:

$$\epsilon_{\rm enc}(z,\rho)=\epsilon_0(\rho)\exp\{-\tfrac{1}{2}[\alpha z-I_0(\rho)+I_{\rm enc}(z,\rho)]\} \tag{11}$$

with

$$\epsilon_0(\rho)=[I_0(\rho)]^{1/2}\ ,\qquad I_{\rm enc}(z,\rho)=\epsilon_{\rm enc}^2(z,\rho)\ . \tag{12}$$

Equation (11) displays the nonuniform absorption. The behavior of $I_{\rm enc}$ as a function of I_0 for given αz was given in I. At a given αz, the profile may be generally distorted in three different manners, depending on ρ:

(a) transparency for $\rho \ll [\frac{1}{2}\ln(I_{0,0}/\alpha z)]^{1/2}$;
(b) nonlinear absorption for $\rho \sim [\frac{1}{2}\ln(I_{0,0}/\alpha z)]^{1/2}$;
(c) uniform absorption for $\rho \gg [\frac{1}{2}\ln(I_{0,0}/\alpha z)]^{1/2}$.

Therefore, in the case we are dealing with, $I_{0,0} \gg \alpha z$ the three regimes exist successively on the beam profile. As the beam propagates through the cell from the entrance, the wings are progressively washed out, first uniformly from $\rho=\infty$, like $e^{-\alpha z}$, then nonlinearly near $\rho=[\frac{1}{2}\ln(I_{0,0}/\alpha z)]^{1/2}$, whereas the near-axis intensity is almost not absorbed.

The nonlinear absorption implies a stripping of the outer edges of the beam profile. This stripping causes the similarity between the on-resonance enhancement and Fresnel diffraction patterns from a circular aperture as mentioned by BS.

This interpretation is different from the usual lensing one: self-focusing in a dispersive medium can be predicted by using a perturbation expansion of the nonlinearity and diffraction interplay from the zeroth-order solution. Such a treatment does not predict any on-axis on-resonance enhancement that confirms the analysis of BS, but it displays an off-axis divergence. The latter feature is proving very useful in defining the circular aperture, by its width and its location in the cell.

The perturbation expansion of the exact solution $\epsilon(z,\rho)$ in powers of the small parameter $1/2F$ is

$$\epsilon(z,\rho)=\epsilon_{\rm enc}(z,\rho)+\frac{i}{2F}\epsilon_1(z,\rho)+\frac{1}{(2F)^2}\epsilon_2(z,\rho)+\cdots\ , \tag{13}$$

where $\epsilon_1,\epsilon_2,\ldots,$ are real functions. They are found to obey the differential equations

$$\frac{\partial}{\partial z}\epsilon_1=\nabla_t^2\epsilon_{\rm enc}-\frac{\epsilon_1}{1+\epsilon_{\rm enc}^2}\ , \tag{14a}$$

$$\frac{\partial}{\partial z}\epsilon_2=-\nabla_t^2\epsilon_1+\epsilon_{\rm enc}\left[\frac{\epsilon_1^2+2\epsilon_{\rm enc}\epsilon_0}{(1+\epsilon_{\rm enc}^2)^2}\right]-\frac{\epsilon_2}{1+\epsilon_{\rm enc}^2}\ , \tag{14b}$$

when putting Eq. (13) into Eq. (9). They lead to the integral equations

$$\epsilon_1(z,\rho)=\epsilon_{\rm enc}(z,\rho)\int_0^z dz'\frac{1}{\epsilon_{\rm enc}(z',\rho)}\nabla_t^2\epsilon_{\rm enc}(z',\rho)\ , \tag{15a}$$

$$\epsilon_2(z,\rho)=\frac{\epsilon_{\rm enc}(z,\rho)}{1+I_{\rm enc}(z,\rho)}\int_0^z dz'\left[-\frac{1+I_{\rm enc}(z',\rho)}{\epsilon_{\rm enc}(z',\rho)}\nabla_t^2\epsilon_1(z',\rho)+\frac{\epsilon_1^2(z',\rho)}{1+I_{\rm enc}(z',\rho)}\right]\ . \tag{15b}$$

The expressions of $\epsilon_1(z,\rho)$ and $\nabla_t^2\epsilon_1(z,\rho)$ are given in the Appendix.

In order to illustrate this perturbation treatment, we have chosen a set of values for $I_{0,0}$ and F, used by BS in their Fig. 2, $\epsilon_{0,0}=10$ and $F=60$. In Fig. 1, the transverse profiles of ϵ_0, ϵ_1, and ϵ_2 are plotted for four successive penetrations. Both corrections $1/2F\epsilon_1$ and $(1/2F)^2\epsilon_2$ in-

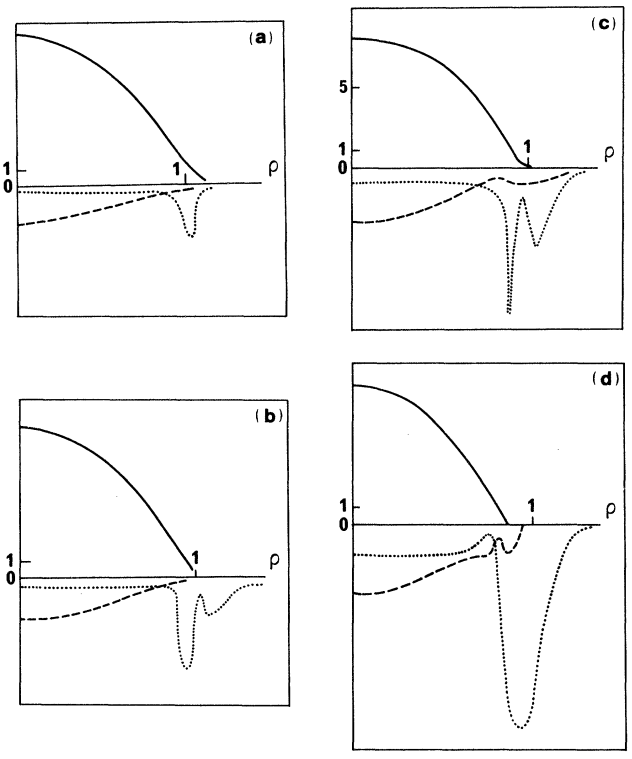

FIG. 1. Three first terms in perturbative expansion [Eq. (5)] with $I_{0,0}=100$, $F=60$, as a function of ρ for various abscissa: (a) $z=0.22z_d$, (b) $z=0.26z_d$, (c) $z=0.33z_d$, (d) $z=0.44z_d$. Solid lines correspond to the encoded field $\epsilon_{\rm enc}$, dashed lines to the first-order correction $\epsilon_1/2F$, and dotted lines to the second-order correction $\epsilon_2/(2F)^2$.

crease with z. The latter exhibits a peak around $\rho \simeq 1$, the height of which increases with z, until it diverges at $z \simeq 0.33 z_d$. Thus the perturbation treatment displays an off-axis enhancement near $z \simeq 0.33 z_d$, from which diffraction is no longer properly described by a perturbation expansion. The penetration $z = 0.22 z_d$, where the perturbation is still valid, corresponds to the beginning of the wing stripping.

The emergence of a divergence on the wing profile can be understood when looking for the behavior of the nonlinear absorption together with the role of the diffraction on ϵ_{enc}. The ρ derivative of the absorption term is easily calculated as

$$\frac{\partial}{\partial \rho}\left[\frac{\epsilon_{\text{enc}}}{1+I_{\text{enc}}}\right] = -2\rho \frac{\epsilon_{\text{enc}}}{(1+I_{\text{enc}})^3}(1+I_0)(1-I_{\text{enc}}) . \quad (16)$$

This expression displays an extremum on the transverse profile of the absorption kernel, for

$$I_{\text{enc}}(z,\rho) = 1 . \quad (17)$$

This identity defines a set of coordinates $\rho_{\text{st}}, z_{\text{st}}$ related via the implicit equation (11) such that

$$\rho_{\text{st}} = \left[-\frac{1}{2} \ln \left[\frac{\alpha z_{\text{st}} + 1 + \rho_{\text{st}}^2 - \ln(1_{0,0})}{I_{0,0}} \right] \right]^{1/2} \quad (18a)$$

or

$$\rho_{\text{st}} \simeq [\tfrac{1}{2} \ln(I_{0,0}/\alpha z_{\text{st}})]^{1/2} . \quad (18b)$$

At location z_{st}, $\rho = \rho_{\text{st}}$ is the radius for which the profile is affected the most by the nonlinear absorption. At z_{st}, does the diffraction work? On the whole profile or only on the neighborhood of ρ_{st}? The effect of the diffraction can be roughly estimated with the help of $\nabla_t^2 \epsilon_{\text{enc}}$:

$$\nabla_t^2 \epsilon_{\text{enc}} = \frac{4\epsilon_{\text{enc}}}{1+I_{\text{enc}}} \left[-(1-\rho^2)(1+I_0) + \rho^2 \frac{(I_0 - I_{\text{enc}})}{1+I_{\text{enc}}} \times \left[1 + I_0 + 2\frac{1 - I_0 I_{\text{enc}}}{1+I_{\text{enc}}} \right] \right] . \quad (19)$$

In both limiting cases of transparency and uniform absorption, $\nabla_t^2 \epsilon_{\text{enc}}$ can be approximated by $-4\epsilon_{\text{enc}}(1-\rho^2)$. Now let us consider the variation of $\nabla_t^2 \epsilon_{\text{enc}}$ with respect to z on the ring of radius ρ_{st}. Before z_{st}, there is almost complete transparency; at z_{st}, defined by Eqs. (17) and (18) $\nabla_t^2 \epsilon_{\text{enc}}$ becomes proportional to I_0,

$$\nabla_t^2 \epsilon_{\text{enc}} \mid_{\rho_{\text{st}}, z_{\text{st}}} \simeq -2\epsilon_{\text{enc}} I_0 (1-2\rho^2) \mid_{\rho_{\text{st}}, z_{\text{st}}} \simeq -2 I_0 (1-2\rho^2) \mid_{\rho_{\text{st}}, z_{\text{st}}} . \quad (20)$$

After I_{enc} reaches unity, encoding (11) shows that a small increment Δz_{st} of magnitude of order $\frac{1}{2}(\Delta z_{\text{st}}/z_{\text{st}}) \sim [I_0(\rho_{\text{st}})]^{-1}$ leads to a decreasing of I_{enc} of approximately $1/e$. Then $\nabla_t^2 \epsilon_{\text{enc}}$ becomes proportional to I_0^2:

$$\nabla_t^2 \epsilon_{\text{enc}} \mid_{\rho_{\text{st}}, z_{\text{st}} + \Delta z_{\text{st}}} \simeq \rho_{\text{st}}^2 I_0^2(\rho_{\text{st}}) . \quad (21)$$

Therefore, just after nonlinear absorption reaches its maximum, diffraction effects suddenly increase as $I_0^2(\rho_{\text{st}})$. Diffraction will prevail on stripping when $(1/2F)\nabla_t^2 \epsilon_{\text{enc}}$ becomes of the order of magnitude of the absorption term, or

$$\nabla_t^2 \epsilon_{\text{enc}} \mid_{z_{\text{st}}, \rho_{\text{st}}} \gtrsim \frac{F \epsilon_{\text{enc}}}{1+I_{\text{enc}}} \mid_{z_{\text{st}}, \rho_{\text{st}}} , \quad (22)$$

i.e., by using Eq. (19) together with $I_{\text{enc}}(z_{\text{st}}, \rho_{\text{st}})$

$$|1 - 2\rho_{\text{st}}^2| \, e^{1-2\rho_{\text{st}}^2} \gtrsim \frac{F}{2I_{0,0}} . \quad (23)$$

This latter relation does exhibit two regimes depending on the ratio $F/I_{0,0}$. Roughly speaking, for any $F/2I_{0,0} \gtrsim 1$, Eq. (22) implies $\rho < 1/\sqrt{2}$, and for $F < 2I_{0,0}$, it needs $\rho_{\text{st}} > 1/\sqrt{2}$. The aperture width decreases as $F/I_{0,0}$ increases. This feature will be shown to be in agreement with the numerical results in Sec. III. A larger $I_{0,0}$ needs a smaller aperture giving rise to more oscillations of the on-axis intensity as the light propagates.

These two regimes correspond to BS2 and BS3, respectively. More precisely, for BS2 ($F = 60$ and $I_{0,0} = 100$), Eq. (22) together with Eq. (18b) leads to

$$\rho_{\text{st}} = 1 , \quad z_{\text{st}} = 0.22 z_d , \quad (24)$$

in agreement with the location of the off-axis divergence shown in Fig. 1.

This description for encoding is valid only if $I_0(\rho_{\text{st}})$ is much greater than unity in order that strong nonlinear absorption works at ρ_{st} (see I). This implies $z_{\text{st}} \gg \alpha^{-1}$. On the other hand, stripping of the beam requires that diffraction is negligible up to z_{st}, i.e., $z_{\text{st}} \ll z_d$. In summary, the conditions of stripping are

$$\alpha^{-1} \ll z_{\text{st}} \ll z_d . \quad (25)$$

The usefulness of the perturbation expansion stops at z_{st}. Afterwards diffraction dominates the absorption process and it must be taken *fully* into account, via the operator $e^{-iz/4z_d \nabla_t^2}$.[14]

III. DIFFRACTION FROM STRIPPED BEAM

We proceed by taking account of diffraction from z_{st}, as discussed in Sec. II. In order to treat it, we assume that diffraction and absorption are uncorrelated processes from z_{st} so that diffraction works as in free space. This approximation is well justified for any $\rho \gtrsim \rho_{\text{st}}$ where I_{enc} is smaller than unity, but it is not so obvious near the axis where nonlinear absorption is expected further in the cell. The effect of the near-axis nonlinear absorption can be actually neglected if both z_{st} and the abscissa of the on-axis maximum, z_M, measured from z_{st}, obey

$$\alpha z_{\text{st}} \ll I_{0,0} , \quad (26a)$$

$$\alpha(z_{\text{st}} + z_M) \ll I_{0,0} . \quad (26b)$$

The application of the diffraction operator $e^{(iz/4z_d)\nabla_t^2}$ on $\epsilon_{\text{enc}}(z_{\text{st}}, \rho)$ is not so obvious. This could be performed in paper I since the beam was stripped on the whole profile. Therefore, we model the stripped amplitude by a truncated Gaussian at $\rho = \rho_{\text{st}}$, as if the beam passes through a cir-

cular aperture at z_{st}. The application of the diffraction operator is more easily handled in Cartesian coordinates, so that the circular aperture is replaced by a square one of full width $2a$.

All approximations considered, the distortion of the amplitude profile will be described by the product $D(x)D(y)$ of the diffraction functions on the Ox axis and Oy axis, with

$$D(x)=e^{(iz/4z_d)(\partial^2/\partial x^2)}U(a-|x|)e^{-x^2}. \tag{27}$$

Equation (27) can be calculated by taking the Fourier transform $\tilde{D}(K_x)$ of $D(x)$ and then performing a convolution product on a finite aperture,

$$D(x)=\frac{1}{\xi}e^{-x^2/\xi^2}\frac{1}{2}\left\{\operatorname{erf}\left[\left[\frac{-iz_d}{z}\right]^{1/2}(a\xi-x/\xi)\right]+\operatorname{erf}\left[\left[\frac{-iz_d}{z}\right]^{1/2}(a\xi+x/\xi)\right]\right\}, \tag{28}$$

$$\xi=\left[1+\frac{iz}{z_d}\right]^{1/2}.$$

Equation (28) exhibits the Fresnel interferences for arbitrary propagation length z. The on-axis diffracted function for the intensity $|D(0)|^4$ is plotted in Fig. 2 as a function of z for two different apertures. It first displays rapid oscillations for very small values of z/z_d and then a distinct wide maximum for an abscissa z_{max}. The wider the aperture, the lower and the further the maximum. When the full width $2a$ increases from 0.2 to 2, the maximum decreases from 3.2 to 1.35 and the abscissa increases from $0.04z_d$ to $0.35z_d$ (see Fig. 3). It follows that both the enhancement of the on-axis intensity and the focus will depend on the choice of the aperture width.

Now, let us compare our model, stripping from 0 to z_{st} followed by diffraction by an aperture of half-width a, with numerical results. The case $\epsilon_{0,0}=10$, $F=60$, in Fig. 2 of Ref. 1 that we labeled BS2 and the other, $\epsilon_{0,0}=15$, $F=500$, in Fig. 3 of Ref. 1 (BS3 case), are shown in Figs. 4(a) and 4(b), respectively. In the three curves, the abscissa origin is z_{st}. The dashed line exhibits the numerical[14] on-axis intensity resulting from direct integration of Eq.

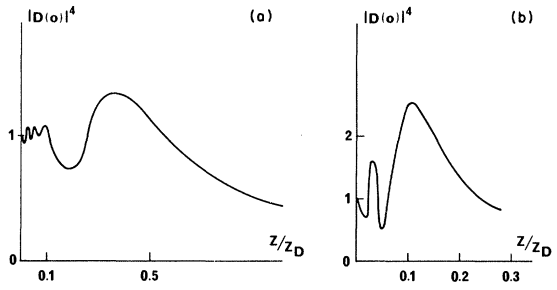

FIG. 2. On-axis diffraction function for the intensity

$$|D(0)|^4=[1/1+(z/z_d)^2]\,|\operatorname{erf}[a(1-iz_d/z)^{1/2}]|^4$$

as a function of z/z_d: (a) $a=1$, (b) $a=0.5$.

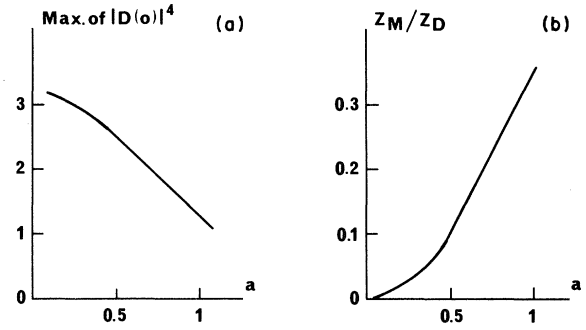

FIG. 3. Role of the aperture width: (a) variation of the maximum of $|D(0)|^4$ as a function of half-width a; (b) variation of the abscissa z_M/z_d as a function of a.

(9) with an input Gaussian profile at $z=0$. The solid line displays $|D(0)|^4$, the diffraction function for the intensity for $a=1$ in Fig. 4(a) and $a=0.8$ in Fig. 4(b). The dotted line exhibits a diffraction function for the intensity without modeling the stripping by an aperture. In this simulation, the beam undergoes stripping from 0 to z_{st} and then only diffraction. Therefore, the dotted line exhibits the effect of the free-space propagation on the *exact* encoded function $\epsilon_{enc}(z_{st},\rho)$ given by Eq. (11).

Solid lines agree well with the dotted ones, with $a=1$ in BS2 and $a=0.8$ in BS3, except at the very beginning where the fast oscillations result from the cutoff. This good agreement confirms that stripping is accounted for quite well by an aperture.

The neglect of absorption in the solid and dotted lines of Fig. 4 explains the discrepancy between them and the exact on-axis intensity (dashed line). In BS2 the exact maximum is below the approximated one: The latter can be corrected by multiplying the solid and the dotted lines by $e^{-\alpha z/I_{0,0}}$; then it gives approximately the accurate enhancement with respect to the input as shown in Table I. The approximate focus for BS2 is located slightly further than the exact one. This discrepancy cannot be generally corrected by changing the width of the aperture. If a decreases, the enhancement increases and z_M decreases (Fig. 3), but in counterpart, z_{st} increases so much that z_f $(=z_{st}+z_M)$ does too. Table I shows a comparison between a numerical simulation and our model for a BS3′ case, with $I_{0,0}=225$ and $F=150$. Conclusions are the same as for BS2.

For BS3, the situation is rather different. The exact maximum is larger than the approximated one, in which absorption was neglected. Table I also illustrates that the model is too crude. As the aperture decreases, the enhancement increases and goes to the exact one, but the position of the focus is unchanged (there is a balance effect between the increasing of z_{st} and the decreasing of z_M). In this case, the inequality (26) is not satisfied. $I_{0,0}$ is only twice αz_M in BS3 whereas it is 5 times αz_M in BS2. In BS3 near-axis nonlinear absorption cannot be neglected after z_{st}.

Finally, in Fig. 5, profiles given by our model $|D(x)D(0)|^2$ are compared with the exact profiles of the intensity. Figure 5(a) displays results for BS2 and Fig.

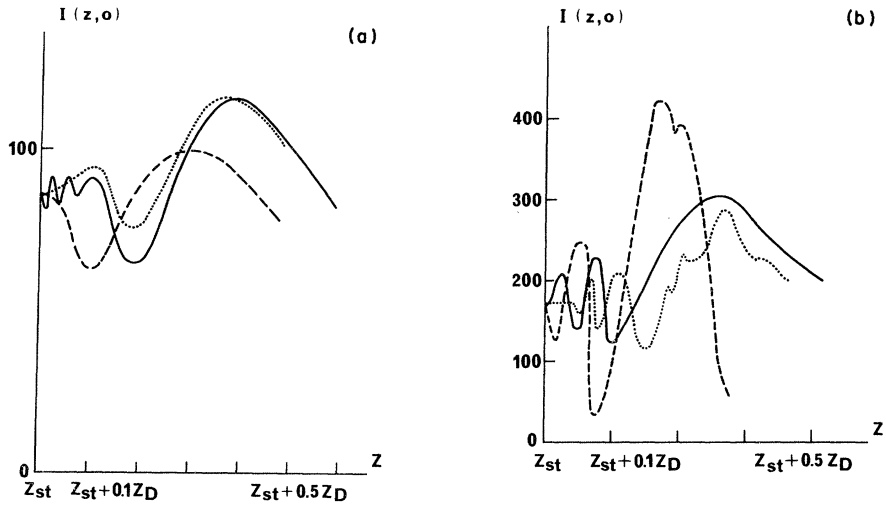

FIG. 4. On-axis intensity behavior as a function of z/z_d from $z_{st}=I_{0,0}e^{-2a^2}$. Solid line [Eq. (28)] corresponds to stripping modeled by an aperture at z_{st}. Dotted line exhibits Fresnel interferences from z_{st} on the numerically calculated stripped amplitude. Absorption is not taken into account in either the solid or dotted lines. Dashed line shows the numerical simulation with absorption included for all z. (a) BS2, $I_{0,0}=100$, $F=60$, $a=1$, $z_{st}=0.22z_d$. (b) BS3, $I_{0,0}=225$, $F=500$, $a=0.8$, $z_{st}=0.125z_d$.

5(b) displays results for BS3. We see that our model displays good enough profiles for BS2 but poor fits for BS3.

IV. CONCLUSION

The perturbation treatment of the diffraction which is a usual and successful treatment in case of self-lensing, does not predict any on-axis enhancement when working on a stripped beam exactly tuned on resonance with atoms. On the contrary, a simple description of wing stripping modeled by a circular aperture, from which the beam is diffracted, reproduces fairly well the numerical results of BS. Such an agreement confirms that the on-axis on-resonance enhancement is a result of Fresnel interferences. As is well known, Fresnel interferences are a consequence of strong diffraction effects and they explain, *a posteriori*, the breakdown of the perturbation treatment of the diffraction.

The aperture model exhibits the main features of the on-axis on-resonance enhancement, especially its variation with $I_{0,0}$ and F. The enhancement, the number, and the relatives heights of the on-axis oscillations increase as $I_{0,0}$ does. In terms of Fresnel interferences this implies that the aperture decreases as $I_{0,0}$ increases, as reproduced in

TABLE I. Comparison between our model for the BS2, BS3′, and BS3 cases with numerical simulation results.

	BS2		BS3′		BS3	
	$I_{0,0}=100$ z_f/z_d	$F=60$ $I_f/I_{0,0}$	$I_{0,0}=225$ z_f/z_d	$F=150$ $I_f/I_{0,0}$	$I_{0,0}=225$ z_f/z_d	$F=500$ $I_f/I_{0,0}$
Numerical simulation[a]	0.52	~ 1	0.4	~ 1.2	0.28	1.8
Encoding plus free-space propagation[b]	0.55	0.9			0.33	0.9
Analytical model[c]						
$a=1$, z_{st} $\begin{cases}0.22z_d(\text{BS2})\\0.06z_d(\text{BS3}-\text{BS3}')\end{cases}$	0.57	0.9	0.41	0.9	0.4	0.5
$a=0.9$, z_{st} $\begin{cases}0.33z_d(\text{BS2})\\0.09z_d(\text{BS3})\end{cases}$	0.63	~ 1	0.39	1		
$a=0.8$, $z_{st}=0.125z_d$					0.4	0.7
$a=0.5$, $z_{st}=0.272z_d$					0.37	1.4
$a=0.4$, $z_{st}=0.327z_d$					0.39	1.5

[a]Numerical simulation $z=0-z_f$ [Eq. (9)] (dashed line, Fig. 5).

[b]Encoding [Eq. (11)] from 0 to z_{st} plus free-space propagation from z_{st} to z_f; $\alpha z_{st}=I_{0,0}/e^2$ (dotted line, Fig. 5).

[c]Analytical model. Encoding approximated by an aperture at z_{st} [$I(z_{st},\rho)\propto I_{0,0}e^{-2a^2}$ for $\rho<a$; $I_{0,0}\propto 0$ for $\rho>a$] plus free-space propagation (solid line, Fig. 5).

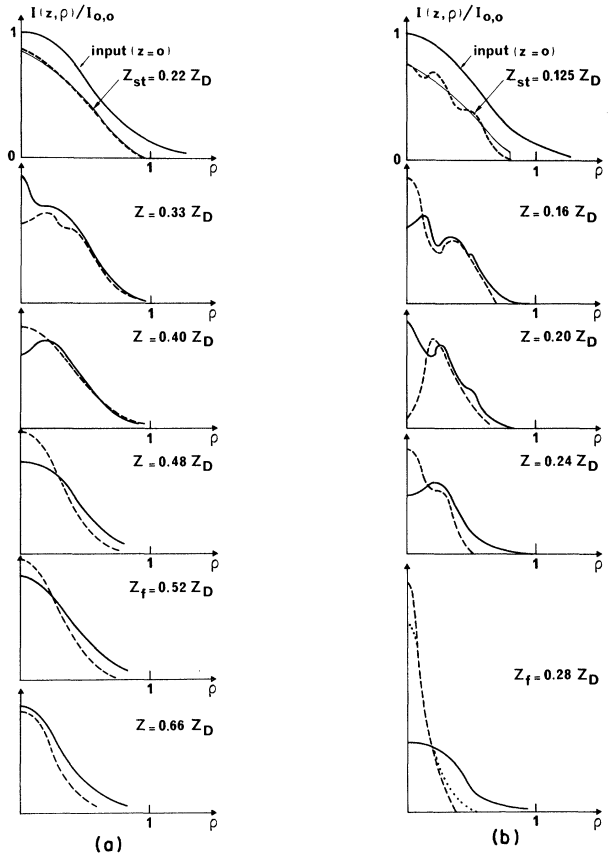

FIG. 5. Transverse shapes of the intensity. Dashed line exhibits numerical simulation. (a) is relative to BS2, solid line shows analytic model with $a=1$. (b) is relative to BS3, solid line shows analytic model with $a=0.8$, dotted line at the focus corresponds to $a=0.4$.

our model [see Eq. (23)]. The higher the input intensity, the smaller the aperture. Furthermore, the aperture model shows that an enhancement is expected for

$$6I_{0,0} \gtrsim F \gg I_{0,0}/e^2 \gg 1 , \tag{29}$$

in agreement with numerical results. The maximum enhancement appears for $F/I_{0,0} \simeq 2$ whatever both F and $I_{0,0}$ may be. When F increases above $2I_{0,0}$, the aperture width decreases [see Eq. (23)]; the amount of energy in the beam at z_{st} decreases so that the enhancement decreases. (In Ref. 10, with $I_{0,0}=225$, the on-axis enhancement is approximately 1.8 at maximum, $F \sim 2I_{0,0}$ and decreases to 1.25 for $F \sim 6I_{0,0}$.) As F goes up further, we find again the case of I.[8(b)] The aperture vanishes as exhibited by Eq. (23) in the limit of large $F/I_{0,0}$. For $F/I_{0,0} \gtrsim 6$, the whole profile is stripped at $z_{st}=z_{NL}$.[8(b)] Reshaping effects result still from Fresnel diffraction but the energy in the core of the beam profile is so small that no enhancement is expected.

The best choice for the observation of an on-resonance enhancement is $F \simeq 2I_{0,0}$. The difficulties to fit both the profiles near the aperture and near the focus in BS3 case do not lie in the concept of an aperture by itself. The weak side of the present model consists in assuming that the undistorted input Gaussian beam goes through an effective aperture. A better model would take successive stripping and diffraction effects into account. In other words, we could imagine that the beam undergoes diffractions by successive apertures with decreasing widths. An improvement of our aperture model in this direction would lead to a better prediction of the on-resonance enhancement. But it would not be probably so easily handled and the simple physical understanding would not gain so much. Doppler broadening could affect the on-resonance enhancement; its effect will be discussed elsewhere.

ACKNOWLEDGMENTS

We are grateful to H. M. Gibbs for illuminating discussions and thank W. J. Sandle for interesting discussions at the fifth coherence and quantum optics conference of Rochester. F.P.M.'s program was partially supported by the U.S. Army Research Office (DAAG 23-79-C0148).

APPENDIX

Integration of Eqs. (14), although not exciting, is straightforward. Let us give $\epsilon_1(z,\rho)$

$$\epsilon_1(z,\rho) = -2\epsilon_{\text{enc}}(1+I_0)\ln\left[\frac{I_0}{I_{\text{enc}}}\right] + 2\epsilon_{\text{enc}}\rho^2\left[[2I_0+(1+I_0)^2]\ln\left[\frac{I_0}{I_{\text{enc}}}\right] - (1+I_0)^2\ln\left[\frac{1+I_0}{1+I_{\text{enc}}}\right] + 2(1+I_0)^2\left[\frac{1}{1+I_0}-\frac{1}{1+I_{\text{enc}}}\right]\right] . \tag{A1}$$

ϵ_2 was calculated with the help of Eqs. [15(b) and A_1]. The analytical expression of the integrand of Eq. 15(b) was numerically integrated over the variable z.

Let us give the analytical expression of $\nabla_t^2\epsilon_1$:

$$\nabla_t^2\epsilon_1 = 4\epsilon_{\text{enc}}(2A_0+2\rho^2A_1+4\rho^4A_4) ,$$

$$A_0 = [(1+I_0)\beta+4I_0+(1+I_0)^2]\ln\frac{I_0}{I_{\text{enc}}} - (1+I_0)^2\ln\beta + 2\beta(I_{\text{enc}}-I_0) ,$$

$$A_1=-[4I_0+6I_0\beta-\beta(1+I_0)+2\beta^3]\ln\frac{I_0}{I_{\rm enc}}-4[2I_0-\beta^2-\beta(2I_0-1)]+6\beta B(\rho)+3\frac{1}{\rho}\frac{\partial}{\partial\rho}B(\rho)\,,$$

$$A_2=\left[-\beta^2+2\beta^2\frac{1}{1+I_{\rm enc}}+\frac{2I_0}{1+I_{\rm enc}}\right]B(\rho)-\beta\frac{1}{\rho}\frac{\partial}{\partial\rho}B(\rho)$$
$$+4I_0\left[2(1+I_0)\ln\frac{I_0}{I_{\rm enc}}-(1+2I_0)\ln\beta+\frac{9}{2}+\frac{7}{2}\beta^2-\frac{(4+7I_0)}{1+I_{\rm enc}}-\beta^2\frac{6}{1+I_{\rm enc}}-\beta^3\frac{1+I_0}{I_0}+\frac{4}{I_0}\beta^4-3\beta^4\frac{I_0}{1+I_{\rm enc}}\right]$$

with

$$\beta=\frac{1+I_0}{1+I_{\rm enc}}\,,$$

$$B(\rho)=\tfrac{1}{2}[2I_0+(1+I_0)^2]\ln\frac{I_0}{I_{\rm enc}}+(1+I_0)^2\left[-\frac{1}{2}\ln\beta+\frac{1}{1+I_0}-\frac{1}{1+I_{\rm enc}}\right]. \tag{A2}$$

[1]M. G. Boshier and W. J. Sandle, Opt. Commun. 42, 371 (1982).

[2]J. Marburger, in *Progress in Quantum Electronics,* edited by J. H. Sanders and S. Stenholm (Pergamon, New York, 1975), Vol. 4, p. 35, and references herein.

[3]A. Yariv, in *Quantum Electronics,* 2nd ed. (Wiley, New York, 1975), p. 498, and references herein.

[4]N. Wright and M. C. Newstein, Opt. Commun. 9, 8 (1975); IEEE J. Quantum Electron. QE-10, 743 (1973).

[5]F. Mattar and M. C. Newstein, Opt. Commun. 18, 70 (1976); in *Cooperative Effects in Matter and Radiation,* edited by C. M. Bowden *et al.* (Plenum, New York, 1977), p. 139.

[6]B. Bolger, L. Baede, and H. M. Gibbs, Opt. Commun. 18, 67 (1976); H. M. Gibbs, B. Bolger, F. P. Mattar, M. C. Newstein, G. Forster, and P. E. Toschek, Phys. Rev. Lett. 37, 1743 (1976).

[7]M. Le Berre, E. Ressayre, and A. Tallet, in *Coherence and Quantum Optics V,* Proceedings of the Fifth Rochester Conference, edited by L. Mandel and E. Wolf (Plenum, New York, in press).

[8](a) M. Le Berre, E. Ressayre, and A. Tallet, in *Proceedings of the International Conference on Laser's 81* (STS, McLean, Virginia, 1981), p. 120; (b) Phys. Rev. A 25, 1604 (1982) (referred to as I).

[9]M. Le Berre, E. Ressayre, A. Tallet, H. M. Gibbs, M. C. Rushford, and F. P. Mattar, in *Coherence and Quantum Optics V,* Proceedings of the Fifth Rochester Conference, edited by L. Mandel and E. Wolf (Plenum, New York, in press).

[10]M. G. Boshier, thesis, University of Otago, Dunedin, New Zealand, 1982.

[11]M. Le Berre, F. P. Mattar, E. Ressayre, and A. Tallet, SPIE J. 369, 269 (1983).

[12]The numerical simulations of Boshier and Sandle were confirmed independently by P. D. Drummond, F. P. Mattar, and K. Tai (private communications).

[13]A. Icsevgi and W. E. Lamb, Jr., Phys. Rev. 185, 517 (1969).

[14]Numerical simulations were performed with a simplified version of F. P. Mattar's program; Appl. Phys. 17, 53 (1978).